

Millimeter Wave Inspection of Titanium Powder

A. Barvincak¹, R. Zoughi¹, P. Collins², K. O'Donnell², J. Zaugg², M. Quintana², J. Johnson³, and D. Palmer³

^{1,2}Center for Nondestructive Evaluation (CNDE)

¹Electrical and Computer Engineering (ECpE) Department
Iowa State University (ISU) - rzoughi@iastate.edu

²Materials Science and Engineering (MSE) Department
Iowa State University (ISU) - pcollins@iastate.edu

³The Boeing Company
Huntsville, AL - jessica.h.johnson@boeing.com

ABSTRACT

Properties of metal powder, used in laser powder bed fusion (LPBF) additive manufacturing (AM) process, is critically important as it pertains to the quality of the final printed part. In this paper, millimeter wave materials characterization is investigated as a potential tool for detecting surface oxidation in titanium powder and contamination by fine graphite powder. Stock titanium powder was exposed to elevated temperatures to promote oxidation. Millimeter wave measurements of oxidized and un-oxidized powder did not indicate a measurable distinction between the two species. However, the technique showed good sensitivity for detecting and evaluating fine graphite powder contamination. This paper outlines the method of oxidation, measurements to obtain oxidation level ground truth data, as well as a brief explanation of the measurement.

Keywords: Titanium powder, additive manufacturing, materials characterization, millimeter waves.

METHODS OF OXIDATION AND MATERIALS CHARACTERIZATION

Millimeter wave frequency range spans 30-300 GHz. Over the past thirty years, a number of robust techniques have been developed addressing a myriad of materials characterization applications and needs [1]. When measuring conducting powder (i.e., metals) the reflection and/or transmission properties of the powder may be directly used to differentiate among powders with different levels of oxidation (i.e., corrosion) [2]. This paper outlines the method by which titanium powder was oxidized and the millimeter wave material characterization technique that was employed to distinguish among virgin, oxidized and contaminated powder species.

Method of Oxidation

A small amount (~500-700 mg; <300 mm³) of powder was placed in an alumina crucible and placed into a furnace under laboratory air. The times/temperatures listed in Table 1 were used for this study. A picture of the powders used in this study (post oxidation) is shown in Figure 1. The change in color is apparent at the higher temperatures.

Characterization Method and Results

The very strong affinity of titanium and its alloys for oxygen forms a native, passivating oxide layer. When present in the form of powder, it is common for many powder companies to introduce a “passivation” step in the manufacturing process, since this passivation helps prevent class D metal fires. This native passivation layer is on the order of 3-10 nm thick. When titanium is exposed to atmosphere and elemental species present, including both oxygen and nitrogen, it can develop layers of oxides and nitrides that can have varying degrees of complexity relating to the crystal structures and chemistries [3]. As the oxides/nitrides grow in thickness, they change color. Color is related to a combination of both thickness and composition of the oxides. To obtain the so-called “ground truth” regarding the oxide thickness layer following the oxidation process, the powder was characterized using a focused ion beam/scanning electron microscope (FIB/SEM) Dual Beam system.

Table 1: Predicted oxygen ingress in hep alpha titanium (pure titanium) as function of time and temperature.

Thickness (unit)	T (C)	Time of experiment (hr)			
		0.5	1	2	4
Alpha	200	3.24 pm	4.58 pm	6.47 pm	9.15 pm
	300	2.79 A	3.95 A	5.58 A	7.89 A
	400	6.40 nm	9.06 nm	12.8 nm	18.1 nm
	500	65.3 nm	92.4 nm	131 nm	184 nm



Figure 1: Powders following oxidation. Each group of 4 represents a temperature, increasing from 200°C (left) to 500°C (right). Within each group of four vials, times increase from left to right (i.e., 0.5, 1.0, 2.0, 4.0 hours). The single vial at the top is the virgin (unoxidized) powder.

Such systems enable advanced characterization including site-specific cross-sectioning of material in a system with concurrent analysis capabilities. Figure 1 shows a through cross-section of a metal particle, providing a “*reference frame*”. We also obtained elemental maps using energy dispersive spectroscopy (EDS). In the end, it was determined that the average induced oxide layer thickness was ~32 nm, which is less than what had been initially predicted.

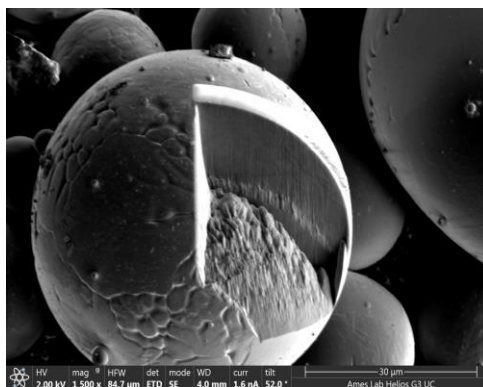


Figure 2: Cross-section through picture of a powder particle.

MILLIMETER WAVE CHARACTERIZATION TECHNIQUE

We employed the millimeter wave materials characterization technique involving an open-ended circular waveguide operating in the TE_{01} mode [4]. Using this technique, the open-ended circular waveguide probe is used to irradiate a thin layer of powder that is housed in a circular conducting hole. Subsequently, the reflected millimeter wave amplitude and phase (or real and imaginary parts) are measured, as complex S_{11} . The measurements were conducted in the 32-40 GHz which is in the Ka-band (25.6-40 GHz) frequency range, accommodating the waveguide operation above cutoff. Figure 3a shows the schematic of the measurement technique, while also showing the magnitude of the electric field in and around the open-ended probe. Figure 3b shows a set of sixteen holes, machined in an aluminum

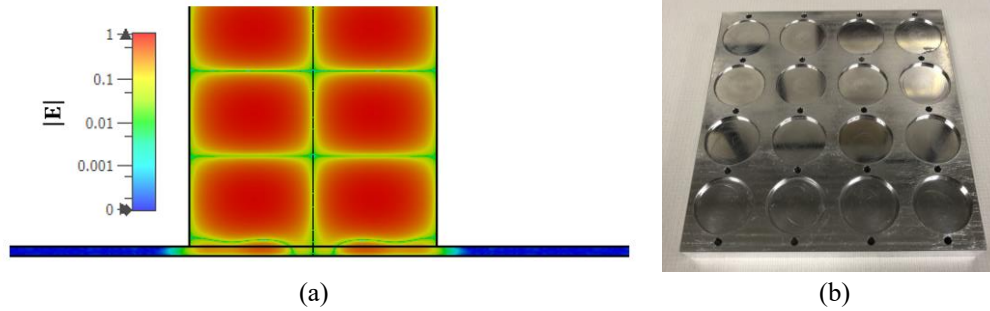


Figure 3: a) Magnitude of electric field distribution in and around an open-ended circular waveguide aperture radiating into a thin, conductor-backed dielectric layer, and b) a set of sixteen holes, machined in an aluminum substrate, with different thicknesses for the open-ended circular waveguide measurements.

substrate, for filling them with powder and each having a different (hole) thickness. Once filled, then the circular waveguide probe irradiates the sample holder (in contact) and the complex reflection coefficient, S_{11} , is measured.

MEASUREMENT RESULTS

Oxidation Results

Figure 4a shows the measured real and imaginary parts of S_{11} (in polar format) for powder samples exposed to 200°C as a function of exposure duration. Each curve starts on the left side representing the lowest measured frequency (i.e., 32 GHz) results and traverses clockwise over frequency all the way to the highest measured frequency (i.e., 40 GHz). The outcomes of the measurements indicate that the measured S_{11} results are practically indistinguishable, which means the level of produced surface oxidation must have been very small not to affect the measurements. Figure 4b shows the same results but for 500°C. The same conclusion can be deduced in this case as well. The results shown in Figure 4 were obtained using the 0.9 mm-thick sample holder. Similar results were obtained for other sample holder depths.

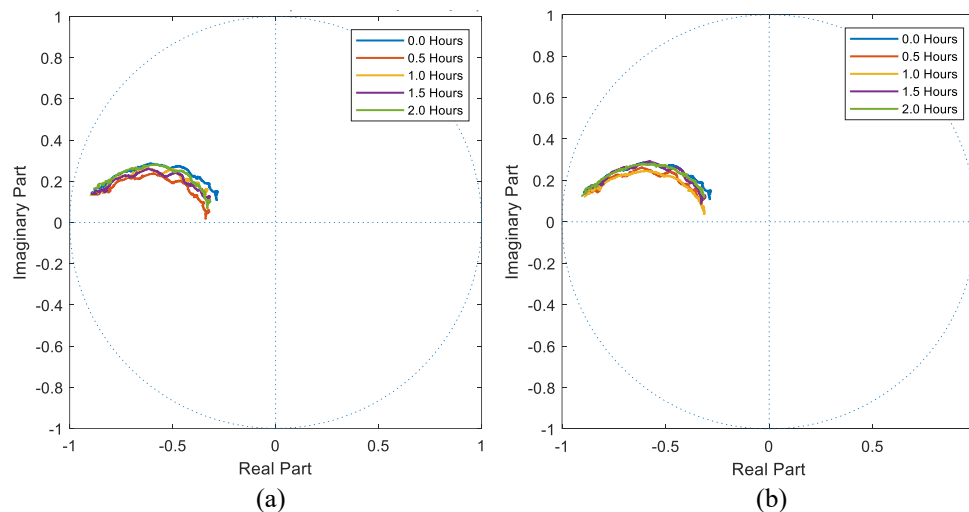


Figure 4: Measured complex S_{11} (in polar format) in the frequency range of 32-40 GHz, for oxidized powder as a function of exposure time: a) at 200°C, and b) 500°C.

Graphite Powder Contamination Results

Using the open-ended circular waveguide technique, we also investigated the potential for detecting small amount of graphite powder contamination in the virgin powder stock. For this purpose, we obtained the commercially-available #205 Graphite powder. According to the datasheet, the #205 Graphite will not be less than 80% Carbon and has a

maximum size for 99.5% of the particles of < 44 microns. Initially, several small amounts of the graphite powder were uniformly mixed with the virgin titanium powder. Seven such samples were produced with the following percentage (by mass) of graphite: 0.55%, 1.0%, 1.78%, 4.79%, 19.96% and 100%, respectively. The measured complex reflection coefficient, S_{11} , as a function of frequency and graphite contamination percentage using the 1.1 mm-deep sample holder, and for the mentioned percentages are shown in Figure 5a, respectively (the percentages shown are rounded). To further indicate the relatively substantial differences among the measured reflection coefficients, S_{11} , characteristics of these samples (as a function of frequency), Figure 5b shows the phase of S_{11} plotted for the 0.9 mm-deep sample holder. The results clearly show the ability to distinguish among these samples particularly as a function of increasing frequency.

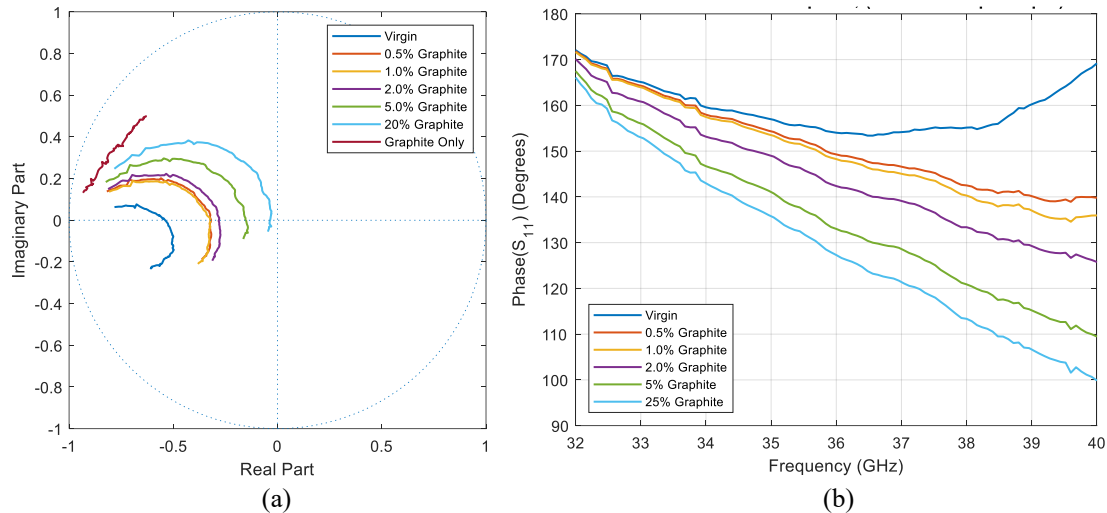


Figure 5: a) Measured complex S_{11} (in polar format) in the frequency range of 32–40 GHz, for different graphite percentages, and b) phase of S_{11} for different graphite percentages as a function of frequency.

SUMMARY

The measurement procedures and results of using a millimeter wave characterization technique, in the 32–40 GHz range, to evaluate oxidized and contaminated (with Graphite powder) titanium powder were presented. The results showed lack of measurement sensitivity to the former, but clear capability for detecting the latter. This work will be further extended to establish the ultimate capabilities of this technique for titanium powder property evaluation.

Acknowledgement – This funding for this work was provided by the Boeing Company.

REFERENCES

1. Brinker, K., M. Dvorsky, M.T. Al Qaseer and R. Zoughi, “Review of Advances in Microwave and Millimeter-Wave NDT&E: Principles and Applications”, *Philosophical Transactions of the Royal Society A: Mathematical, Physical and Engineering Sciences*, A 378: 20190585, p. 29, September 2020.
2. Filbert, J., M.T. Al Qaseer and R. Zoughi, “Microwave Material Characterization of Metal Powder used in Additive Manufacturing,” Presented at the 16th International Symposium for Nondestructive Characterization of Materials, Baltimore, MD, August 10–12, 2021 (virtual).
3. Brice, D.A., P. Samimi, I. Ghamarian, Y. Liu, R.M. Brice, R.F. Reidy, J.D. Cotton, M.J. Kaufman and P.C. Collins, “Oxidation Behavior and Microstructural Decomposition of Ti-6Al-4V and Ti-6Al-4V-1B Sheet,” *Corrosion Science*, vol. 112, pp. 338–346, 2016.
4. Dvorsky, M., M.T. Al Qaseer and R. Zoughi, “Multimodal Solution for a Circular Waveguide Radiating into Multilayered Structures using the Axially-Symmetric TE and TM Modes,” *IEEE Open Journal of Instrumentation & Measurement*, pp. 1–13, May 2023, [DOI:[10.1109/OJIM.2023.3280489](https://doi.org/10.1109/OJIM.2023.3280489)].